

Barium Stars - Theoretical Interpretation

Laura Husti^{A,B,E}, Roberto Gallino^A, Sara Bisterzo^A, Oscar Straniero^D, and Sergio Cristallo^D

^A Dipartimento di Fisica Generale, Università degli Studi di Torino,
via P. Giuria 1, 10125 Torino, Italia

^B Research Centre for Atomic Physics and Astrophysics, University of Bucharest,
P.O.Box MG-6, RO-077125 Bucharest-Magurele, Romania

^D INAF Osservatorio Astronomico di Collurania, via M. Maggini, 64100 Teramo, Italy

^E Email: lotesileanu@yahoo.com

Abstract: Barium stars are extrinsic Asymptotic Giant Branch (AGB) stars. They present the s-enhancement characteristic for AGB and post-AGB stars, but are in an earlier evolutionary stage (main sequence dwarfs, subgiants, red giants). They are believed to form in binary systems, where a more massive companion, evolved faster, produced the s-elements during its AGB phase, polluted the present barium star through stellar winds and became a white dwarf. The samples of barium stars of Allen & Barbuy (2006) and of Smiljanic et al. (2007) are analysed here. Spectra of both samples were obtained at high-resolution and high S/N. We compare these observations with AGB nucleosynthesis models using different initial masses and a spread of ^{13}C -pocket efficiencies. Once a consistent solution is found for the whole elemental distribution of abundances, a proper dilution factor is applied. This dilution is explained by the fact that the s-rich material transferred from the AGB to the nowadays observed star, is mixed with the envelope of the accretor. We also analyse the mass transfer process, and obtain the wind velocity for giants and subgiants with known orbital period. We find evidence that thermohaline mixing is acting inside main sequence dwarfs and we present a method for estimating its depth.

Keywords: stars: abundances — stars: AGB and post-AGB — (stars:) binaries: general — stars: chemically peculiar — stars: mass loss

1 Introduction

Barium stars have been a fascinating subject since their discovery by Bidelman & Keenan (1951). Understanding their peculiar abundance patterns has been a challenge for over 50 years.

Barium stars show s-process enhancement. However, these stars are giants or main-sequence, far away from the thermal pulse asymptotic giant branch stars (TP-AGB) phase, where the s-process is manufactured. Late on the TP phase, AGB stars undergo recurrent third dredge-up (TDU) episodes, mixing with the envelope C-rich and s-process-rich material synthesised in the He intershell (the zone between H shell and He shell). The most likely interpretation of barium stars is that they acquired the s-enrichment by mass transfer in a binary system through stellar winds from an AGB companion that became later on a white dwarf (in some cases detectable, see Boffin & Jorissen 1988, Jorissen & Mayor 1988 and references therein). The study of barium stars is important for a better understanding of the s-process in AGB stars, of the mass transfer in binary systems and of the mixing processes, like thermohaline mixing, which may occur in the envelope of main sequence stars (Stancliffe et al. 2007 and references therein). This is a process that occurs when the mean molecular weight of the stellar material increases towards the surface. The heavier material

transferred from the AGB will sink until the difference in molecular gradient weight will disappear.

A recent homogeneous sample of 26 barium stars with lead measurement detected at high-resolution spectroscopy (S/N ~ 100 to 250) has been analysed by Allen & Barbuy (2006). About half of these stars are barium dwarfs, and half are barium subgiants and giants. Many heavy elements have been observed, among which, Sr, Y, Zr, belonging to the first s-process peak (ls, light-s, at neutron magic number $N = 50$), Ba, La, Ce, Pr, Nd, Sm, belonging to the second s-peak (hs, heavy-s, at $N = 82$). Moreover, for the first time, Pb at the termination of the s-process ($N = 126$), was detected. Similar high-quality spectra (with higher S/N ~ 500) for other 8 barium giants has been analysed by Smiljanic et al. (2007), without lead measurement. The aim of this paper is to compare our theoretical predictions with Allen & Barbuy (2006) and Smiljanic et al. (2007) observational samples.

In Section 2 we present the models used. In Section 3 we compare our theoretical predictions with the observations and we discuss in detail the case of a barium dwarf (HD 123585) and of a barium giant (HD 27271). In Section 4 we perform mass transfer calculations for some stars with known orbital period. These results allow us to check the self-consistency of the dilution factor obtained for giants (or subgiants) and to estimate the depth of the thermohaline mixing for barium

dwarfs.

2 Theoretical models

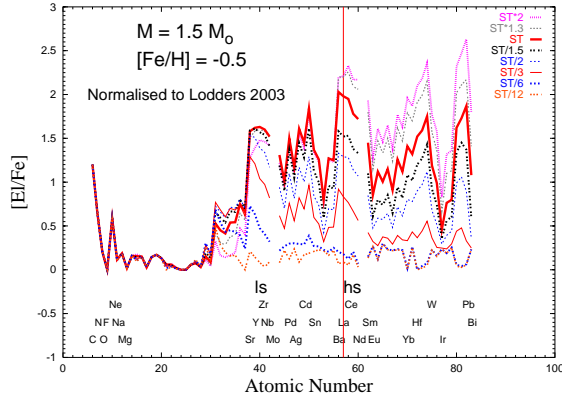


Figure 1: Theoretical predictions of $[El/Fe]$ for AGB models of $M = 1.5 M_{\odot}$, $[Fe/H] = -0.5$ and various ^{13}C -pocket efficiencies (from $ST \times 2$ down to $ST/12$). We normalised to the photospheric values by Lodders (2003).

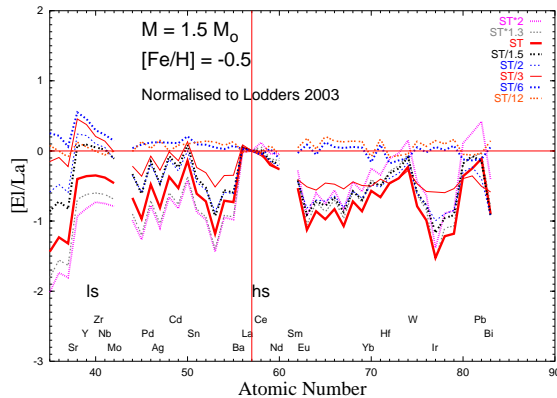


Figure 2: Theoretical predictions $[El/La]$ for elements from Sr to Bi for AGB models of $M = 1.5 M_{\odot}$, $[Fe/H] = -0.5$ and various ^{13}C -pocket efficiencies (from $ST \times 2$ down to $ST/12$).

Our models are based on FRANEC (Frascati Raphson-Newton Evolutionary Code, Chieffi & Straniero 1989), coupled with a post-process code that includes a full network up to bismuth. According to FRANEC, TDU starts after a limited number of TPs. TDU ceases when the mass of the envelope decreases by mass loss down to $\sim 0.5 M_{\odot}$. The TDU mass per pulse reaches a maximum after about ten thermal pulses and then decreases (Straniero et al. 2003). The major neutron source in AGB stars is the $^{13}\text{C}(\alpha, n)^{16}\text{O}$ reaction, which releases neutrons in radiative conditions during the interpulse phase (Straniero et al. 1995). During TDU, a small amount of protons is assumed to penetrate in the top layers of the He intershell. At H reig-

nition, protons are captured by the abundant ^{12}C , via $^{12}\text{C}(p, \gamma)^{13}\text{N}(\beta^+ \nu)^{13}\text{C}$. We use AGB models having initial masses of 1.4, 1.5, 2 and $3 M_{\odot}$, different metallicities and a range of ^{13}C -pocket efficiencies, from $ST \times 2$ down to $ST/12$. Case ST is the standard choice of Gallino et al. (1998), which was shown to best reproduce the solar main component of the s-process (Arlandini et al. 1999). The $ST \times 2$ case roughly corresponds to the maximum ^{13}C -pocket efficiency. Higher proton abundances would lead to the formation of ^{14}N at expenses of ^{13}C . Moreover, ^{14}N would act as a major neutron poison. We may define a minimum ^{13}C -pocket as the one that significantly affects the final s-process distribution. This limit corresponds roughly to $ST/6$ at solar metallicity and decreases with decreasing metallicity, given that the neutron exposure is inversely proportional to the iron seeds. A second minor neutron source is driven by the reaction $^{22}\text{Ne}(\alpha, n)^{25}\text{Mg}$, partially activated during TPs, producing a neutron burst of small neutron exposure and high peak neutron density. For a detailed description of the models we refer to Busso, Gallino & Wasserburg (1999) and Straniero et al. (2003).

As barium stars owe their s-enhancement to mass transfer, the s-rich material from the AGB donor was mixed and diluted with the envelope of the future barium star. Defining the dilution factor as $M_{\star}^{env}/M_{\text{AGB}}^{transf} = 10^{dil}$, where M_{\star}^{env} is the mass of the envelope of the observed star after the mass transfer, M_{AGB}^{transf} is the mass transferred from the AGB, we obtain the diluted theoretical abundances¹:

$$\left[\frac{X}{Fe}\right] = \log \left(10^{\left[\frac{X}{Fe}\right]^{ini}} \cdot f + 10^{\left[\frac{X}{Fe}\right]^{AGB}} \cdot 10^{-dil} \right), \quad (1)$$

where $f = 1 - 10^{-dil}$ and $[X/Fe]^{AGB}$ is the abundance of the element X in the AGB. We suppose that the two stars formed from the same cloud of interstellar gas.

Dilution will lower the abundances of the elements, but will not change the shape of the s-process distribution. If $dil \simeq 0$, it means that no mixing had occurred after the mass transfer, and the observed abundances are the same as in the AGB star.

We present in Fig. 1 theoretical predictions for elements from carbon to bismuth using AGB models of $1.5 M_{\odot}$ and $[Fe/H] = -0.5$ at the last TDU episode for a range of ^{13}C -pocket efficiencies. Note that about half of the AGB mass ejected by stellar winds has a chemical composition shown in the Figure. Indeed, as recalled in Section 2, according to FRANEC, TDU ceases when the envelope mass is of the order of $0.5 M_{\odot}$. The same results are shown in Fig. 2 for heavier elements normalised to lanthanum, which is the best representative element of the hs peak.

3 Results

The Allen & Barbuy (2006) sample contains both dwarfs and barium giants or subgiants. Barium dwarfs have

¹The standard spectroscopic notation is adopted: $[A/B] = \log_{10}(N_A/N_B)_{\star} - \log_{10}(N_A/N_B)_{\odot}$.

negligible convective envelopes. In order to estimate the mass of convective envelope of our sample stars, we used the Window To The Stars (WTTS) interface to Peter Eggletons TWIN single and binary stellar evolution code (Izzard & Glebbeek 2006). Giants and subgiants have larger convective envelopes and some of the giants have already suffered the first dredge-up (FDU), so we expect large dilution factors in these cases.

In order to find a possible solution for a barium star, we seek for the ^{13}C -pocket efficiency that would reproduce the observed trend for the elements belonging to the three s-peaks, ls, hs and Pb. We define

$$[\text{ls}/\text{Fe}] = \frac{([\text{Y}/\text{Fe}] + [\text{Zr}/\text{Fe}])}{2} \quad (2)$$

and

$$[\text{hs}/\text{Fe}] = \frac{([\text{La}/\text{Fe}] + [\text{Nd}/\text{Fe}] + [\text{Sm}/\text{Fe}])}{3} \quad (3)$$

and their ratios $[\text{hs}/\text{ls}]$ and $[\text{Pb}/\text{hs}]$, two s-process indexes independent of the dilution factor.

In Fig. 3–5, we compare spectroscopic observations of the barium dwarf HD 123585 and the barium giant HD 27271 by Allen & Barbuy (2006)².

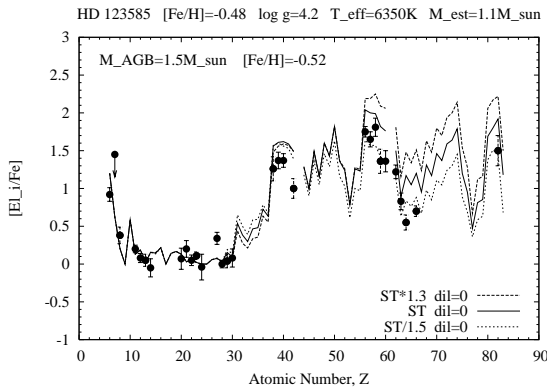


Figure 3: The barium dwarf star HD 123585 elemental spectroscopic distribution compared with theoretical predictions. We plot the theoretical abundances without dilution, for an AGB with initial mass $M_{\text{AGB}} = 1.5 M_{\odot}$, $[\text{Fe}/\text{H}] = -0.52$ and three different ^{13}C -pocket efficiencies (ST, $\text{ST} \times 1.3$ and $\text{ST}/1.5$).

HD 123585 is a **barium dwarf** of metallicity $[\text{Fe}/\text{H}] = -0.48$ with orbital period of 458 days (Pourbaix & Jorissen 2000). The s-enhancement is quite

²The errorbars in the plots are quoted from Allen & Barbuy (2006) and represent the highest value between the uncertainty due to the atmospheric model together with the stellar parameters and the line-to-line scatter for elements with more than two lines used to derive the abundances. These errorbars are plotted as solid lines. For elements where the abundances were derived from only one or two lines (O, 2 lines; Sr, 1 line for dwarfs, 2 lines for giants; Pb, 1 line; Mo, 1 line) we have plotted with dashed line the errorbar. This value has to be considered as a lower limit of the uncertainty for the abundances of these elements.

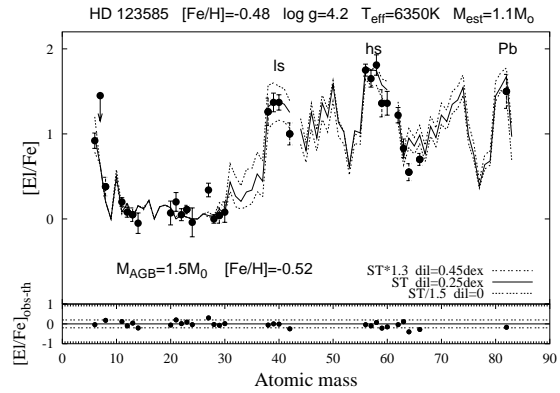


Figure 4: The barium dwarf star HD 123585 elemental spectroscopic distribution compared with theoretical predictions. We plot the theoretical abundances with dilution, for the $1.5 M_{\odot}$ AGB model with $[\text{Fe}/\text{H}] = -0.52$ and three ^{13}C -pocket efficiencies (ST, $\text{ST} \times 1.3$ and $\text{ST}/1.5$).

large: $[\text{ls}/\text{Fe}] \sim 1.4$ dex, $[\text{hs}/\text{Fe}] \sim 1.7$ dex and $[\text{Pb}/\text{Fe}] \sim 1.5$ dex. For HD 123585, the ST case (the solid line in Fig. 3) satisfies this condition: in the theoretical case $[\text{hs}/\text{ls}] = 0.14$ and $[\text{Pb}/\text{hs}] = 0.17$, while from the observations we have $[\text{hs}/\text{ls}]$ and $[\text{Pb}/\text{hs}]$ respectively 0.07 and 0.13, with a typical uncertainty of 0.2 dex. For the other two cases plotted in Fig. 3, $\text{ST} \times 1.3$ and $\text{ST}/1.5$, the discrepancy in $[\text{hs}/\text{ls}]$, with respect to the observational values is ~ 0.4 dex for the $\text{ST} \times 1.3$ case, and ~ 0.3 dex for the $\text{ST}/1.5$ case. The dilution factor dil is then chosen in order to match the $[\text{hs}/\text{Fe}]$ predictions with spectroscopic data. In Fig. 4 we notice that, after dilution, all the three cases shown ($\text{ST} \times 1.3$, ST and $\text{ST}/1.5$) match the hs-peak, but only the ST case matches the ls-peak.

Very similar solutions are obtained with the ST case and an initial mass of the AGB donor of 2 and $3 M_{\odot}$. The dilution factor is 0.25 dex for the $1.5 M_{\odot}$ model, 0.6 dex for the $2 M_{\odot}$ model and 0.5 for the $3 M_{\odot}$ model. Mo, Gd and Dy, each derived from 1 line, are lower than expected. Note that our relative s-process expectations of close-by elements are quite robust and are based on accurate neutron capture cross sections.

HD 27271 is a **barium giant** of solar metallicity with orbital period of 1694 days (Udry et al. 1998a). For this star $[\text{ls}/\text{Fe}] \sim 1$, $[\text{hs}/\text{Fe}] \sim 0.5$ and $[\text{Pb}/\text{Fe}] \sim 0.3$ dex. We were able to reproduce the observations using a case $\text{ST} \times 1.3$, and dilution factors 0.1, 0.3 and 0.45 dex for models with $M = 1.5, 2$ and $3 M_{\odot}$, respectively. The solution found for the $1.5 M_{\odot}$ initial mass of the AGB donor was discarded, because the estimated mass of this star is $M_{\text{est}} = 1.9 M_{\odot}$ (Allen & Barbuy 2006). Mo, with only one line detected, appears too low.

In Table 1, the major characteristics of the Allen & Barbuy (2006) sample are shown. For each star, we report the effective temperature, luminosity, $\log g$, the metallicity, the estimated mass of the star, the con-

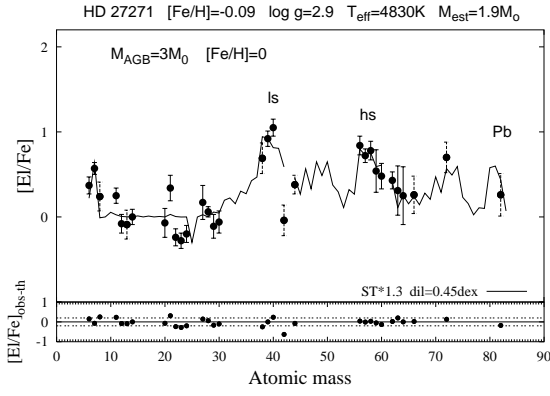


Figure 5: Barium giant HD 27271. Fit obtained with an AGB model of $3 M_{\odot}$ initial mass, $[\text{Fe}/\text{H}] = 0$, $\text{ST} \times 1.3$ ^{13}C -pocket efficiency and 0.45 dex dilution.

vective envelope mass according to FRANEC (see also Izzard & Glebbeek 2006), and the parameters used to obtain the theoretical fits (efficiency of the ^{13}C -pocket, initial mass of the AGB, dilution factor and reduced χ -squared χ^2 to evaluate the goodness of the fit). Note as, in general, the adopted ^{13}C -pocket does not change with the initial AGB mass (Col. 9). The only exception is HD 76225, with a case ST for a model $M = 1.5 M_{\odot}$ and ST/1.5 for models $M = 2$ and $3 M_{\odot}$. For the two giants HD 749 and HD 12392, a dilution of about 0.5 dex can be obtained by decreasing the metallicity by about 0.2 dex.

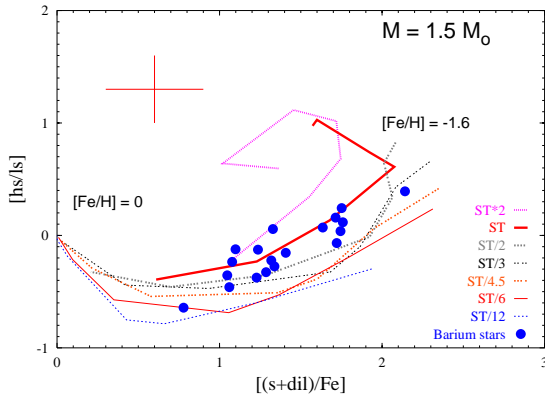


Figure 6: Theoretical results for $[\text{hs}/\text{ls}]$ versus $[(s+\text{dil})/\text{Fe}]$ (where dil is the dilution factor), using AGB models of initial mass $M_{\text{ini}}^{\text{AGB}} = 1.5 M_{\odot}$ and a range of ^{13}C -pocket efficiencies. Full circles correspond to spectroscopic observations of barium stars of the Allen & Barbuy (2006) sample. For higher ^{13}C -pocket efficiencies and decreasing the metallicity, $[(s+\text{dil})/\text{Fe}]$ decreases because the s-process feeds mostly Pb.

In Fig. 6 we show theoretical predictions of $[\text{hs}/\text{ls}]$ versus $[(s+\text{dil})/\text{Fe}]$ for AGB models of $M = 1.5 M_{\odot}$. Here ' s/Fe ' means $([\text{ls}/\text{Fe}] + [\text{hs}/\text{Fe}])/2$ and 'dil' is the

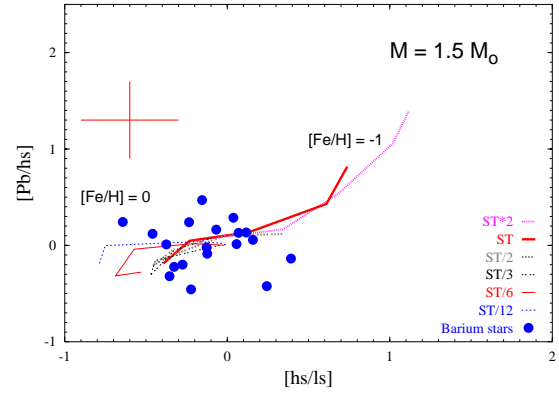


Figure 7: The same as Fig. 6, but for $[\text{Pb}/\text{hs}]$ versus $[\text{hs}/\text{ls}]$.

dilution factor used in the model. Stars interpreted with a $M_{\text{ini}}^{\text{AGB}} = 1.5 M_{\odot}$ are represented with full circles (see Table 1, Cols. 10 and 11). Typical errorbars are shown. Similarly, in Fig. 7, we shown theoretical predictions as compared with observations of $[\text{Pb}/\text{hs}]$ versus $[\text{hs}/\text{ls}]$. $[\text{Pb}/\text{hs}]$ shows quite a large scatter with respect to predictions, due to the fact that only one line of Pb has been detected.

For more detailed descriptions on the other stars we refer to Husti PhD Thesis (2008), and to the preliminary analyses by Husti & Gallino (2008) and Husti, Gallino & Straniero (2008).

Smiljanic et al. (2007) analysed a sample of 8 classical and mild barium giants, known in the literature, reanalysed at high-resolution and S/N. The estimated mass is in the range 1.9 to $4.2 M_{\odot}$ and the metallicity ranging from solar down to $[\text{Fe}/\text{H}] \sim -0.3$. For most of these giants, only one line was detected for Sr and Sm, and two lines for Nd. For these elements no errorbars are given by the authors. Y, Zr, La and Ce are better determined. The quoted errorbars are typically higher in the Smiljanic et al. (2007) sample than in Allen & Barbuy (2006), despite higher S/N spectra. No lead abundances were determined. A preliminary analysis of the two barium stars HD 116713 and HD 205011 has been presented by Husti & Gallino (2008). In Table 3, we show the main characteristics of this sample, with their theoretical interpretations, in particular, our $[\text{Pb}/\text{Fe}]$ predictions. For the two stars HD 46407 and HD 204075, a dilution of 0.7 dex and $[\text{Pb}/\text{Fe}] \sim 1.4$ would be obtained by decreasing the metallicity by ~ 0.2 dex. All stars have a typical $[\text{hs}/\text{ls}]$ close to 0. The only exception is HD 139195 for which $[\text{hs}/\text{ls}] \sim 0.25$.

4 Mass transfer calculations

Boffin & Jorissen (1988) showed that the amount of mass transferred from an AGB star to its companion through stellar winds (ΔM_2) depends on the present value of the orbital separation, the mass of the barium

star and of the white dwarf companion:

$$\Delta M_2 = \frac{1}{\sqrt{1-e^2}} \left[\frac{GM_2}{V_{wind}^2} \right]^2 \frac{\alpha}{2A} \Delta M_1 \times \left[\frac{1}{1 + G(M_1 + M_2)/AV_{wind}^2} \right]^{3/2}, \quad (4)$$

where M_1 is the mass of the white dwarf, M_2 the mass of the barium star, ΔM_1 is the mass lost by winds by the AGB companion, A is the semi-major axis, α is a free parameter put equal to 2 (Boffin & Jorissen 1988) and e the eccentricity. The semi-major axis A varies with the mass exchange between the two binaries. A choice $A = \text{constant}$ may be considered an acceptable approximation during the superwind phase at the end of the AGB. Our FRANEC models adopt the Reimers (1977) mass loss formula and do not explicitly include superwinds, however we recall that almost $0.5 M_\odot$ of the envelope mass is ejected with the same s-process composition.

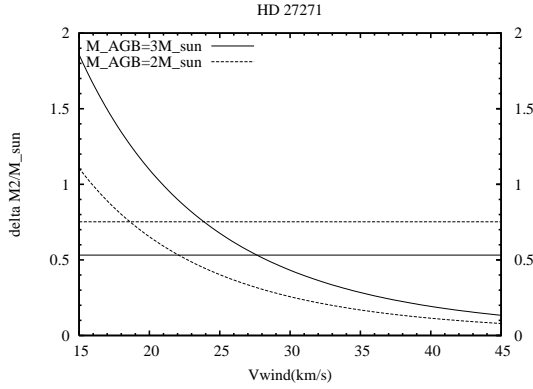


Figure 8: Transferred mass onto the barium giant HD 27271 versus wind velocity.

Thus knowing the mass of the convective envelope from FRANEC and the dilution factor obtained from the abundance fits we may derive the velocity of the wind, for the giants and subgiants, of which we know the orbital period, by comparing ΔM_2 from the equation above with M_{AGB}^{transf} from Section 2.

In Fig. 8 we plot ΔM_2 ($\equiv M_{AGB}^{transf}$) as a function of the wind velocity and the value of M_{AGB}^{transf} ($\equiv \Delta M_2$) obtained from the dilution factor used to get the fit. For HD 27271 we obtain 2 solutions: $V_{wind} \simeq 23$ km/s if we consider the initial mass of the AGB to be $3 M_\odot$, and $V_{wind} \simeq 18$ km/s if we consider the initial mass of the AGB to be $2 M_\odot$. The wind velocity for AGB stars was estimated to be in the interval 20 – 40 km/s (Knapp 1985; Pottasch 1984). Only the solution obtained for the $3 M_\odot$ case is in this range.

Half of the sample are barium dwarfs. The range of estimated mass of dwarfs by Allen & Barbuy (2006) is between $0.9 \leq M_{est}/M_\odot \leq 1.4$. No convective envelope is expected for these objects. Many of the stars need dilution factor higher than 0.5 dex. This might be explained by moderate to strong thermohaline mixing.

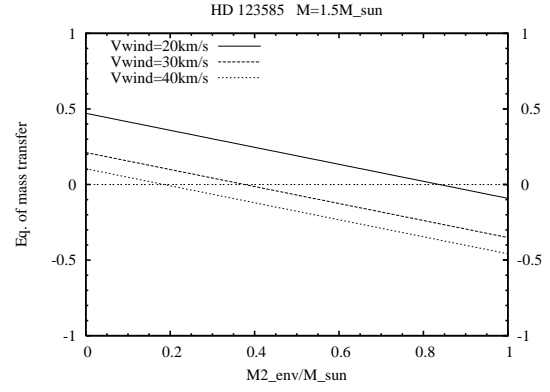


Figure 9: Equation of the mass transfer versus mass of the envelope mixed with the s-enhanced material, for star HD 123585, the case of the $1.5 M_\odot$ initial AGB mass of the companion.

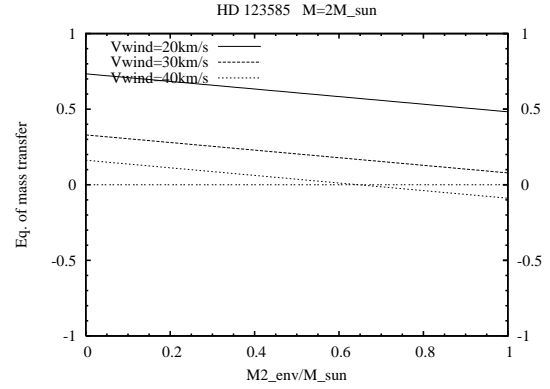


Figure 10: Equation of the mass transfer versus mass of the envelope mixed with the s-enhanced material, for star HD 123585, the case of the $2 M_\odot$ initial AGB mass of the companion.

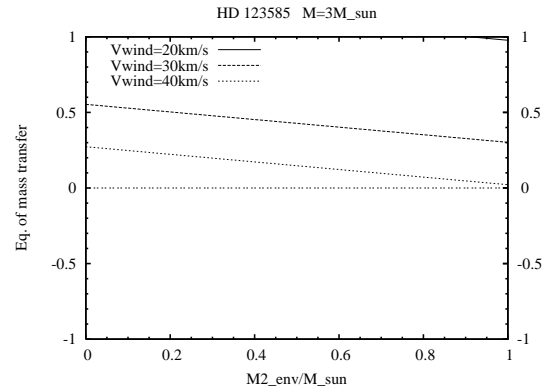


Figure 11: Equation of the mass transfer versus mass of the envelope mixed with the s-enhanced material, for star HD 123585, the case of the $3 M_\odot$ initial AGB mass of the companion.

Putting to zero the mass transfer equation, and replacing ΔM_2 with $M_{env}^{dil}/10^{dil}$, we may estimate the depth of the mixing. In Figs 9, 10 and 11, we have plotted the equation of mass transfer versus the amount of envelope mass over which the s-rich material is diluted due to thermohaline mixing, for HD 123585. In the 2 and 3 M_\odot cases, the depth of the mixing (in mass) would exceed the mass of the barium star for $V_{wind} = 20$ km/s, so we discard these cases. For the 1.5 M_\odot , the amount of envelope mass mixed with the s-rich transferred material is in the range of ~ 0.20 and $\sim 0.85 M_\odot$.

In Table 4 we report the period and the eccentricity available in the literature for six of the barium stars of our sample (Udry et al. 1998a,b – HD 5424, HD 22589, HD 27271 and Pourbaix & Jorissen 2000 – HD 89948, HD 107574, HD 123585), as well as the calculated wind velocity for giants (or subgiants), having various masses of the AGB donor. For HD 5424 we obtain two solutions in the range of 20–40 km/s, for HD 25589 and HD 27271 we have only one solution in the given range, while for HD 107574 we have no solution in the chosen interval, the closest one is for a 1.5 M_\odot AGB companion, with $V_{wind} = 42$ km/s.

In Tables 5 and 6 we present the depth in mass of the thermohaline mixing for the two dwarf stars of the sample with known orbital period. The depth of the mixing depends on the mass of the AGB and on the assumed wind velocity. For HD 89948 we obtain similar results as for HD 123585. The mixing seems to be deeper for the lower metallicity star.

5 Conclusions

We have found theoretical interpretations for the abundance patterns of 26 barium dwarfs, barium subgiants and giants from Allen & Barbuy (2006) and of 8 barium giants from Smiljanic et al. (2007). In order to obtain these solutions, we have applied various dilution factors (from 0 to 1.5 dex) due to the mixing of the s-enhanced material with the envelope of the accretor. In most cases, we have not found unique solutions: models having the same metallicity and ^{13}C -pocket efficiency, but different masses and dilution factors match just as well the observations.

For barium giants and subgiants that have large convective envelopes, an appreciable dilution factor has to be expected, as confirmed by our results. For several barium dwarfs that do not have a convective envelope, an important dilution factor must also be applied. This comes as a proof that efficient thermohaline mixing is active in these stars (Stancliffe et al. 2007).

We have performed some mass transfer calculations for the stars that have the orbital period reported in literature. For barium giants and subgiants we could thus obtain the stellar wind velocity, while for barium dwarfs, assuming a certain initial mass of the AGB and a certain value of the wind velocity, we could estimate the depth of the thermohaline mixing.

Further observations of barium stars with high-resolution spectra and S/N would be very helpful.

Acknowledgments

We thank the referee Rob Izzard for his incisive suggestions to improve the paper. Work supported by the Italian MIUR–PRIN 2006 Project ‘Late Phases of Stellar Evolution: Nucleosynthesis in Supernovae, AGB Stars, Planetary Nebulae’.

References

- Allen, D.M., Barbuy, B., 2006, A&A, 454, 895
- Arlandini, C., Käppeler, F., Wisshak, K., Gallino, R., Lugaro, M., Busso, M., Straniero, O. 1999, ApJ, 525, 886
- Bidelman, W.P., Keenan, P.C., 1951, ApJ, 114, 473
- Boffin, H.M.J., Jorissen, A., 1988, A&A, 205, 155
- Busso, M., Lambert, D. L., Beglio, L., Gallino, R., Raiteri, C. M., Smith, V. V. 1995, ApJ, 446, 775
- Busso, M., Gallino, R., Wasserburg G.J., 1999, ARAA, 37, 239
- Busso, M., Gallino, R., Lambert, D. L., Travaglio, C., Smith, V.V. 2001, ApJ, 557, 802
- Chieffi, A., & Straniero, O. 1989, ApJs, 71, 47
- Gallino, R., Arlandini, C., Busso, M., et al., 1998, ApJ, 497, 388
- Husti, L. (2008), PhD Thesis, "Theoretical interpretation of Barium Stars", Turin University
- Husti, L. & Gallino R. 2008, AIP Conference Proceedings, 1001, 139
- Husti, L., Gallino, R., & Straniero, O. 2008, AIP Conference Proceedings, 990, 161
- Knapp, R., 1985, ApJ, 293, 273
- Izzard, R.G., Glebbeek, E., 2006, New Astronomy, 12, 161
- Lodders, K. 2003, ApJ, 591, 1220
- Jorissen, A. & Mayor, M. 1988, A&A, 198, 187
- Pottasch, S.R., 1984, *Planetary Nebulae*, Astrophys. and Sp. Sci. Library, 106
- Pourbaix, D. Jorissen, A., 2000, A&AS, 145, 161
- Reimers, D. 1977, A&A, 61, 217
- Smiljanic, R., Porto de Mello, G.F., da Silva, L. 2007, A&A, 468, 679
- Stancliffe, R. J., Glebbeek, E., Izzard, R. G., Pols, O. R. 2007, A&A, 464, 57
- Straniero, O., Gallino, R., Busso, M. et al. 1995, ApJ, 440, 85

Table 1: Stellar parameters and results for the Allen & Barbuy (2006) sample. $\bar{\chi}^2$ is calculated for the s-process elements Y, Zr, La, Nd, Sm and Pb. The highest values are principally due to the lead uncertainty.

Stars	T_{eff}	$\log T_{\text{eff}}$	$\log (L/L_{\odot})$	$\log g$	[Fe/H]	M^{est}/M_{\odot}	$M_{\text{obs}}^{\text{env}}/M_{\odot}$	CASE	$M=1.5M_{\odot}$		$M=2.0M_{\odot}$		$M=3.0M_{\odot}$	
									dil	χ^2	dil	χ^2	dil	χ^2
HD 749	4610	3.663	1.322	2.8	-0.06	1.2	0.9	ST \times 1.3	-	-	-	-	0	2.7
HR 107	6440	3.808	0.623	4.08	-0.36	1.2	0	ST \times 1.3	0.9	1.5	1.2	1.3	1.3	1.1
HD 5424	4570	3.659	2.264	2	-0.55	1.9	1.6	ST	-	-	0.8	3.7	0.7	3.3
HD 8270	5940	3.773	0.204	4.2	-0.42	0.9	0	ST/2	0.5	1.0	0.8	1.0	0.7	1.6
HD 12392	5000	3.698	1.301	3.2	-0.12	2	1.5	ST \times 2	-	-	-	-	0	5.6
HD 13551	5870	3.768	0.361	4	-0.44	0.9	0	ST/2	0.4	1.0	0.7	1.5	0.7	1.2
HD 22589	5400	3.732	1.204	3.4	-0.27	1.6	0.5	ST/2	-	-	0.4	2.9	0.5	2.5
HD 27271	4830	3.683	1.505	2.9	-0.09	1.9	1.5	ST \times 1.3	-	-	0.3	1.5	0.45	1.5
HD 48565	5860	3.767	0.397	4.01	-0.62	0.9	0	ST	0.6	0.4	0.9	0.5	0.8	0.5
HD 76225	6110	3.786	0.903	3.8	-0.31	1.4	0	ST-ST/1.5	0.2	3.6	0.2	1.6	0.2	2.6
HD 87080	5460	3.737	0.698	3.7	-0.44	1.2	0.1	ST	0.4	2.5	0.7	2.6	0.7	2.0
HD 89948	6010	3.778	0.204	4.3	-0.3	1	0	ST/1.5	0.2	1.7	0.5	0.8	0.5	0.8
HD 92545	6210	3.793	0.698	4	-0.12	1.3	0	ST \times 2	0.5	1.7	0.7	1.3	0.8	1.9
HD 106191	5890	3.770	0.278	4.2	-0.29	1	0	ST/1.5	0.3	2.2	0.6	2.2	0.6	3.2
HD 107574	6400	3.806	1.113	3.6	-0.55	1.4	0.3	ST	0.8	2.7	1.1	3.0	1.0	2.8
HD 116869	4720	3.673	1.944	2.2	-0.32	1.2	0.9	ST \times 2	1.0	0.6	1.2	0.6	1.3	0.6
HD 123396	4360	3.639	2.406	1.4	-1.19	0.8	0.45	ST/4.5	1.0	3.9	1.2	4.0	-	-
HD 123585	6350	3.802	0.447	4.2	-0.48	1.1	0	ST	0.25	0.7	0.6	0.3	0.5	0.7
HD 147609	5960	3.775	0.079	4.42	-0.45	1	0	ST/2	-	-	0.2	1.6	0.1	2.1
HD 150862	6310	3.800	0.041	4.6	-0.10	1.1	0	ST \times 1.3	0	8.8	0.2	10.0	0.3	9.0
HD 188985	6090	3.784	0.278	4.3	-0.3	1.1	0	ST	0.2	1.2	0.5	1.1	0.6	1.7
HD 210709	4630	3.665	1.681	2.4	-0.04	1.1	0.9	ST \times 2	0.5	0.8	0.7	0.6	0.9	0.5
HD 210910	4570	3.659	1.278	2.7	-0.37	1	0.7	ST/1.5	0.4	4.7	0.7	4.4	0.8	4.1
HD 222349	6130	3.787	0.698	3.9	-0.63	1.2	0	ST	0.6	1.1	0.9	1.1	0.8	1.2
BD +185215	6300	3.799	0.477	4.2	-0.53	1.1	0	ST/2	0.3	4.6	0.6	4.5	0.6	2.9
HD 223938	4970	3.696	1.255	3.1	-0.35	1.4	1.1	ST	0.4	3.6	0.7	3.2	0.8	3.1

Table 2: [ls/Fe], [hs/Fe], [Pb/Fe] and their ratios [hs/ls] and [Pb/hs] for the Allen & Barbuy (2006) sample.

Stars	[Fe/H]	[ls/Fe]	[hs/Fe]	[Pb/Fe]	[hs/ls]	[Pb/hs]
HD 749	-0.06	1.32	1.17	0.38	-0.14	-0.79
HR 107	-0.36	0.59	0.43	0.90	-0.16	0.47
HD 5424	-0.55	1.19	1.51	1.10	0.32	-0.41
HD 8270	-0.42	0.98	0.70	0.50	-0.28	-0.20
HD 12392	-0.12	1.29	1.52	1.15	0.24	-0.37
HD 13551	-0.44	1.05	0.72	0.50	-0.33	-0.22
HD 22589	-0.27	0.95	0.36	-0.15	-0.59	-0.51
HD 27271	-0.09	0.97	0.55	0.31	-0.41	-0.24
HD 48565	-0.62	1.10	1.22	1.35	0.12	0.13
HD 76225	-0.31	1.22	0.84	0.85	-0.38	0.01
HD 87080	-0.44	1.23	1.47	1.05	0.24	-0.42
HD 89948	-0.30	1.03	0.67	0.35	-0.36	-0.32
HD 92545	-0.12	0.70	0.46	0.70	-0.24	0.24
HD 106191	-0.29	0.99	0.53	0.65	-0.46	0.12
HD 107574	-0.55	0.96	0.89	1.05	-0.07	0.16
HD 116869	-0.32	0.64	0.79	0.85	0.16	0.06
HD 123396	-1.19	0.95	1.34	1.20	0.39	-0.14
HD 123585	-0.48	1.35	1.42	1.55	0.07	0.13
HD 147609	-0.45	1.57	1.35	0.78	-0.22	-0.57
HD 150862	-0.10	1.10	0.46	0.70	-0.64	0.24
HD 188985	-0.30	1.10	0.97	0.95	-0.13	-0.02
HD 210709	-0.04	0.66	0.54	0.45	-0.12	-0.09
HD 210910	-0.37	0.45	0.57	-0.04	0.12	-0.61
HD 222349	-0.63	1.13	1.16	1.45	0.04	0.29
BD +185215	-0.53	1.13	0.91	0.45	-0.22	-0.46
HD 223938	-0.35	0.90	0.96	0.97	0.06	0.01

Table 3: Stellar parameters and results for the Smiljanic et al. (2007) sample.

Stars	[Fe/H]	T_{eff}	$\log g$	M_{est}	CASE	$M=3M_{\odot}$ dil	$M=4M_{\odot}$ dil	[Pb/Fe] _{th}
HD 46407	-0.09	4940	2.65	2.3	ST×2	0.2	-	1.1
HD 104979	-0.35	4920	2.58	2.3	ST×1.3	1.4	-	0.6
HD 116713	-0.12	4790	2.67	1.9	ST×2	0.5	-	0.8
HD 139195	-0.04	4910	2.41	2.4	ST	0.8	-	0.0
HD 181053	-0.35	4920	2.58	2.2	ST	1.7	-	0.2
HD 202109	-0.04	4910	2.41	3.0	ST×2	1.5	-	0.2
HD 204075	-0.09	5250	2.49	4.2	ST×2	-	0.3	1.2
HD 205011	-0.14	4780	2.41	2.2	ST×1.3	0.6	-	0.4

Table 4: Parameters of the theoretical solutions. Calculated wind velocities for giants and subgiants.

Stars	P (days)	e	$M_{\text{AGB}}=3M_{\odot}$	$M_{\text{AGB}}=2M_{\odot}$	$M_{\text{AGB}}=1.5M_{\odot}$
			V_{wind} (km/s)	V_{wind} (km/s)	V_{wind} (km/s)
HD 5424	1881	0.225	32	-	-
HD 22589	5721	0.240	22	17	-
HD 27271	1694	0.217	23	18	-
HD 89948	668	0.117	-	-	-
HD 107574	1350	0.081	>45	>45	42
HD 123585	458	0.062	-	-	-

Table 5: HD 89948. Depth of the thermohaline mixing.

HD 89948	$M_{\text{AGB}} = 1.5M_{\odot}$	$M_{\text{AGB}} = 2M_{\odot}$	$M_{\text{AGB}} = 3M_{\odot}$
$V_{\text{wind}} = 20 \text{ km/s}$	0.5	>1	>1
$V_{\text{wind}} = 30 \text{ km/s}$	0.22	0.7	>1
$V_{\text{wind}} = 40 \text{ km/s}$	0.10	0.3	0.55

Table 6: HD 123585. Depth of the thermohaline mixing.

HD 123585	$M_{\text{AGB}} = 1.5M_{\odot}$	$M_{\text{AGB}} = 2M_{\odot}$	$M_{\text{AGB}} = 3M_{\odot}$
$V_{\text{wind}} = 20 \text{ km/s}$	0.83	>1	>1
$V_{\text{wind}} = 30 \text{ km/s}$	0.37	>1	>1
$V_{\text{wind}} = 40 \text{ km/s}$	0.18	0.65	>1

Straniero, O., Domínguez, I., Cristallo, S., Gallino, R.
2003, PASA, 20, 389

Udry, S., Jorissen, A., Mayor, M., et al., 1998a, A&AS,
131, 25

Udry, S., Mayor, M., Van Eck, S., et al., 1998b, A&AS,
131, 43